Communication: Evaporation – Influence of heat transport in the liquid on the interface temperature and the particle flux

Matthias Heinen,[1] Jadran Vrabec,[1,a)] and Johann Fischer[2]

[1]*Lehrstuhl für Thermodynamik und Energietechnik, Universität Paderborn, Warburger Str. 100, 33098 Paderborn, Germany*

[2]*Institut für Verfahrens- und Energietechnik, Universität für Bodenkultur, Muthgasse 107, 1190 Wien, Austria*

Molecular dynamics simulations are reported for the evaporation of a liquid into vacuum, where a Lennard-Jones type fluid with truncated and shifted potential at 2.5σ is considered. Vacuum is enforced locally by particle deletion and the liquid is thermostated in its bulk so that heat flows to the planar interface driving stationary evaporation. The length of the non-thermostated transition region between the bulk liquid and the interface L_n is under study. First, it is found for the reduced bulk liquid temperature $T_l/T_c = 0.74$ (T_c is the critical temperature) that by increasing L_n from 5.2σ to 208σ the interface temperature T_i drops by 17% and the evaporation flux decreases by a factor of 4.4. From a series of simulations for increasing values of L_n, an asymptotic value T_i^∞ of the interface temperature for $L_n \to \infty$ can be estimated which is 21% lower than the bulk liquid temperature T_l. Second, it is found that the evaporation flux is solely determined by the interface temperature T_i, independent on T_l or L_n. Combining these two findings, the evaporation coefficient α of a liquid thermostated on a macroscopic scale is estimated to be $\alpha \approx 0.14$ for $T_l/T_c = 0.74$.

Studies of evaporation were started by Hertz[1] and subsequently a large number of experimental[2-14], theoretical[15-20] and molecular simulation[21-29] works as well as review articles[30-32] and books[33-37] appeared of which only some are cited here. Despite these efforts it still seems that the experimental findings diverge from the existing molecular modelling[17-20] and simulation[21-29] results. On the theoretical side, modelling of evaporation was made for a long time with the kinetic theory of gases, assuming a half-sided Maxwell-Boltzmann velocity distribution function f^+ as a boundary condition for the evaporating gas[17-19] based on the bulk liquid temperature T_l and the corresponding saturated vapor density ρ''. The crucial problem with these approaches, however, is whether such a half-sided Maxwell-Boltzmann velocity distribution function is a physically justified assumption. In order to clarify that problem, non-equilibrium molecular dynamics (NEMD) simulations[21-29] and kinetic theory[20] were applied which include the liquid, the interfacial region and the vapor.

a) Electronic address: jadran.vrabec@upb.de

One aspect of evaporation from a thermostated bulk liquid into vacuum which is not yet fully understood is the transition region between the thermostated liquid and the interface through which, according to Bošnjaković[15], the heat required for evaporation is transported. As a consequence, there must be a temperature drop from the temperature of the thermostated bulk liquid T_l to the temperature of the liquid at the interface boundary T_{li} and further to the temperature of the vapor-liquid interface T_i. Let for the following be T_c the critical temperature of the fluid, σ the molecular size parameter to which all lengths are reduced if no confusion can occur, z the direction perpendicular to the planar interface and L_n the length of the non-thermostated transition region.

Different assumptions were made for L_n in work based on the kinetic theory of fluids or NEMD simulations. Frezzotti et al.[20] specified $L_n \approx 16$ and obtained with kinetic theory linearly decreasing temperature profiles and linearly increasing density profiles from the bulk liquid to the onset of the interface. For $T_l/T_c = 0.729$ the temperature went down to $T_{li}/T_c = 0.676$ and for $T_l/T_c = 0.596$ the temperature went down to $T_{li}/T_c = 0.590$. In their NEMD simulations, Lotfi et al.[21,22] used $L_n \approx 6$ and Ishiyama et al.[25] used $L_n \approx 3$ for $T_l/T_c = 0.73$ which are rather short distances. Most attention to the non-thermostated region was paid by Anisimov et al.[24] They first discussed the heat flux to the interface on a thermodynamic basis. Next, they showed decreasing temperature and increasing density profiles in the non-thermostated region from simulations for $T_{li}/T_c = 0.69$ and 0.80 (Figures 2 and 3 in Ref. 24) with gradients given in Table II. Unfortunately, the length L_n is not clearly stated in that article[24] but from their Figure 3 we estimate $L_n \approx 10$. Finally, regarding the paper of Cheng et al.,[27] we find in their Figure 4 ($T_l/T_c = 0.83$) results starting with a non-stationary transition from equilibrium to evaporation and thereafter quasi-stationary evaporation. A further discussion of that paper[27] is given below.

Stimulated by the ideas of Bošnjaković[15] on the heat transport from the bulk liquid region to the interface, experimental studies[3-14] were made to determine the length L_n and the temperature drop $\Delta T = T_l - T_{li}$. A major difference between experimental work and molecular model calculations,[20-29] however, is the length of the non-thermostated region L_n. Whilst the molecular models assumed $L_n \approx 10^1$, experimental findings[3] are $L_n \approx 1$ mm, corresponding to $\approx 10^6$ in units of σ. Hence, we decided to investigate by NEMD simulations the influence of L_n on the temperatures T_{li} and T_i and subsequently the effect of T_i on the evaporation flux.

Molecular model and simulation method

The model fluid consisted of $\approx 10^6$ to $\approx 3.5 \cdot 10^6$ particles that interact via the truncated and shifted Lennard-Jones potential u_{TS} with a cut-off radius of 2.5σ, where σ is the size parameter, ϵ the energy parameter and m the particle mass.

The potential is defined by

$$u_{TS}(r_{ij}) = \begin{cases} u_{LJ}(r_{ij}) - u_{LJ}(2.5\sigma), & r_{ij} < 2.5\sigma, \\ 0 & r_{ij} > 2.5\sigma, \end{cases} \tag{1}$$

where u_{LJ} is the usual Lennard–Jones potential

$$u_{LJ}(r_{ij}) = 4\epsilon \left[\left(\frac{\sigma}{r_{ij}}\right)^{12} - \left(\frac{\sigma}{r_{ij}}\right)^{6} \right], \tag{2}$$

and r_{ij} is the distance between two molecules i and j.

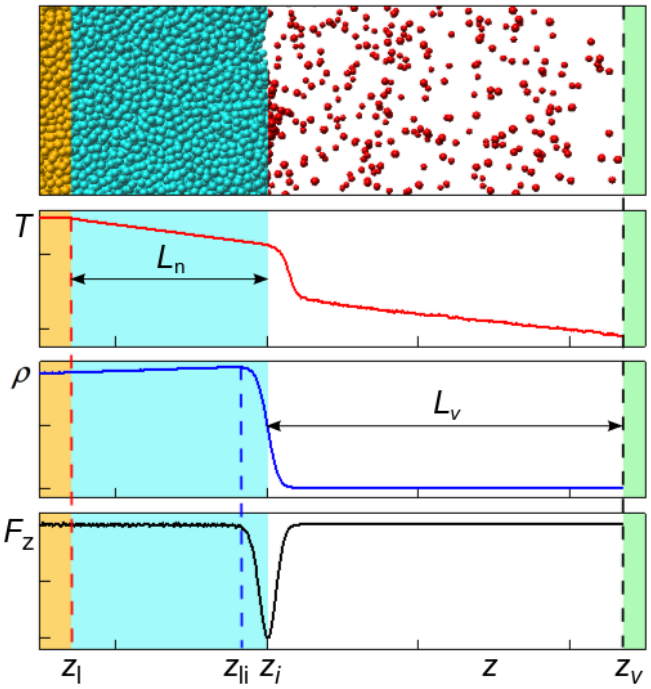

FIG. 1. Position, distance and region definitions for the present stationary evaporation simulations. Thermostating was carried out exclusively in the bulk liquid region (orange), i.e. for $z < z_l$. Vacuum was enforced by removing all particles that have reached the vacuum region (green). The interface plane ($z_i = 0$) between liquid (blue) and vapor (white) is assumed at the minimum of the mean force component in z-direction F_z.

Temperatures are given in units $T^* = Tk/\epsilon$ and evaporation fluxes in units of $j^* = j \cdot \sigma^3\sqrt{m/\epsilon}$ omitting the asterisk. Note that the present investigations are independent on the choice of the parameters σ, ϵ/k and m, where $k = 1.38065 \cdot 10^{-23}$ J/K is the Boltzmann constant. Molecular dynamics simulations were carried out in a cuboid volume with dimensions $L_x = L_y = 140$ and $L_z = 250$ to 550. The system size, i.e. length L_z and number of particles, was adapted to the value of L_n, such that the stationary evaporation process could be maintained for at least 10^6 time steps for production sampling. It was ensured that the width of the thermostating region at the end of data acquisition was still broad enough (> 20). The *ls1*

mardyn code[38] was used for sampling, which is well suited for massively parallel computation. After an equilibration of 10^6 time steps $\Delta t\sigma^{-1}\sqrt{\epsilon/m} = 0.00182$ at a temperature of $T = 0.8$, a liquid slab was formed in the center of the simulation volume that was surrounded by vapor. Because of symmetry reasons, data from both halves of the simulation volume were averaged. The interface plane was defined by the minimum of the mean force component in z direction and was taken as the origin of the z axis, i.e. $z_i = 0$; the temperature there was assumed to be the interface temperature T_i. The resulting saturated vapor and liquid densities agreed well with data from the literature.[39-43] Then evaporation was initiated by removing all particles that propagated into the vapor beyond a distance $L_v = 52$ from the interface. To drive evaporation, the bulk liquid phase with a distance L_n from the interface was thermostated by dividing it into bins with a thickness $\Delta z = 0.5$ which were independently kept at constant temperature by velocity scaling.[44] Position and distance definitions are depicted in Figure 1 in relation to typical temperature, density and force profiles during stationary evaporation. Initially, the system was transient and after $\approx 5 \cdot 10^5 \Delta t$ the evaporation process had reached a steady state.

Because evaporated particles were taken out of the system in the vacuum region and were not re-inserted into the liquid phase, the vapor-liquid interfaces receded over time towards the center of the simulation volume. The coordinate system, however, remained attached to the interface plane and the vacuum distance L_v as well as the length of the non-thermostated region L_n were kept constant. To maintain a constant driving force, the boundary positions of all control regions were updated continuously during simulation. Since all distances are related to the interface positions, they were estimated every 5000th time step by means of the density profile averaged over this time period.

Results and Discussion

First, simulations were performed at constant bulk liquid temperature $T_l = 0.8$ for increasing lengths of the non-thermostated region $L_n = 5.2, 10.4, 15.6, 26, 52, 104$ and 208. Profiles for the kinetic temperatures T_{xy} and T_z, the kinetic energy e, the density ρ, and the evaporation flux j following previous definitions[22] are shown in Figure 2. It can be seen that there is a massive influence of L_n on all of these quantities.

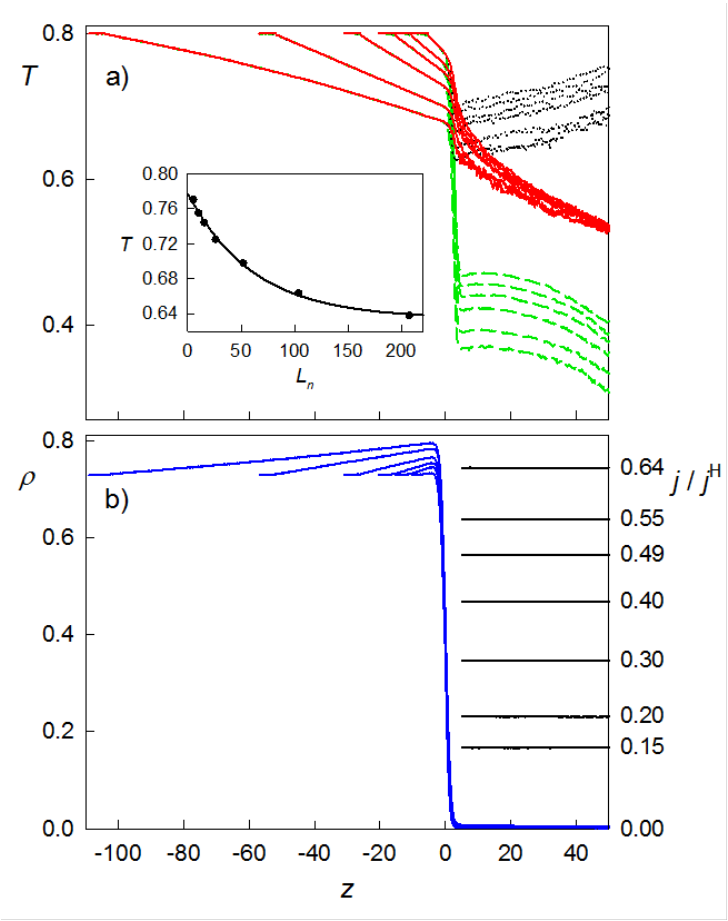

FIG. 2. Profiles obtained at $T_l = 0.8$ for different lengths of the non-thermostated region $L_n = 5.2, 10.4, 15.6, 26, 52, 104$. For better visibility, profiles for $L_n = 208$ are omitted here but are shown in the supporting information. a) Temperature components T_{xy} (solid red), T_z (dashed green) and kinetic energy e (dotted black lines) which coincide in the liquid up to the interface boundary. The inset shows the interface temperature T_i vs. L_n. Bullets indicate simulation data and the line shows correlation (3). b) Density ρ (blue) and evaporation flux j (black lines) normalized to the Hertz flux j^H for $T_i = 0.8$.

In the liquid, the quantities T_{xy}, T_z and e are identical and simply coincide with the temperature T which drops down nearly linearly from T_l to its value at the liquid boundary T_{li} which decreases with increasing L_n, whereas the gradient $\partial T/\partial z$ becomes significantly flatter. The density ρ increases in the non-thermostated region towards the interface and reaches a maximum at a point which we call the boundary of the liquid at the interface. As we believe now that the increase of ρ is due to the decrease of the temperature, the maximum of ρ increases with the length L_n.

On the basis of these data, it is possible to give the hitherto missing physical explanation for the profiles of the temperature, the kinetic energy and the density of Cheng et al.[27] in their Figure 4 ($T_l = 0.90$ or $T_l/T_c = 0.83$). Their profiles show from right to left results for equilibrium, for the transition from equilibrium to evaporation, and for quasi-stationary evaporation states. The crucial point in their simulations is that with increasing time the length of the non-thermostated

region L_n decreases from ≈ 95 to ≈ 35 during quasi-stationary evaporation which is the explanation for the shape of their profiles in the light of the present Figure 2a).

From the temperature profiles shown in Figure 2a) it is clear that with increasing L_n the interface temperature T_i decreases having a dramatic consequence on the evaporation flux j_z which drops down from $L_n = 5.2$ to $L_n = 208$ by a factor of 4.4. Details concerning the interface temperature T_i are given in the inset plot of Figure 2a) and Table I. Because the plot shows that the variation of the interface temperature flattens with increasing length L_n, an asymptotic limiting value T_i^∞ can be expected for $L_n \to \infty$. Hence, a simple correlation is suggested that yields the interface temperature T_i as a function of the length of the non-thermostated region L_n

$$T_i(L_n) = T_i^\infty + b \cdot exp(-cL_n). \tag{3}$$

In addition to b and c, also the limiting temperature of the interface T_i^∞ was an adjustable parameter of Eq. (3). The parameters and results of Eq. (3) are given in Table I and indicate a reasonable asymptotic behavior of the interface temperature T_i, yielding $T_i^\infty = 0.6349$. Employing Eq. (3) to extrapolate the interface temperature and from that the particle flux that can be expected for $L_n \approx 3.5$, a value that Ishiyama et al.[25] used for their calculations, shows that the present data agree with their results for a temperature of $T_l/T_c = 0.74$ within a few percent.

A second study should clarify whether the evaporation flux and the vapor properties are solely determined by the interface temperature T_i, provided that the distance to the vacuum L_v is constant. To elucidate this issue, simulations with three different lengths of the non-thermostated region $L_n = 5.2, 10.4$ and 15.6 were carried out, where the liquid bulk temperature T_l of the simulations with $L_n = 10.4$ and 15.6 was sought by trial and error until almost the same interface temperature T_i was achieved as for the simulation with $T_l = 0.8$ and $L_n = 5.2$, which served as the reference case.

TABLE I. Interface temperature T_i and evaporation flux j at $T_l = 0.8$ for different lengths L_n. T_i^{corr} was calculated from Eq. (3) with $T_i^\infty = 0.6349$, $b = 0.1436$ and $c = 0.01635$. $j^H(T_i^{sim})$ was calculated with the Hertz model[1] for the interface temperature T_i^{sim} and the corresponding saturated vapor density[39] $\rho''(T_i^{sim})$.

L_n	T_i^{sim}	T_i^{corr}	$j^{sim} \cdot 10^3$	$j^H(T_i^{sim}) \cdot 10^3$	$j^{sim}/j^H(T_i^{sim})$
5.2	0.7705	0.7668	4.539	5.299	0.857
10.4	0.7554	0.7560	3.890	4.540	0.857
15.6	0.7444	0.7462	3.443	4.043	0.852
26	0.7251	0.7289	2.856	3.269	0.874
52	0.6981	0.6964	2.119	2.386	0.888
104	0.6637	0.6612	1.417	1.548	0.916
208	0.6382	0.6398	1.029	1.107	0.929

The results shown in Table II indicate that the evaporation flux j depends exclusively on the interface temperature. Moreover, it was conjectured[16] that the evaporation flux j is just the Hertz flux[1,22,24] $j^H(T_i)$ calculated with T_i and the saturated vapor density $\rho''(T_i)$. A comparison of the calculated values for $j^H(T_i)$ with the flux from present simulations j^{sim} is given in Table I. It can be seen that the simulation data for j^{sim} are between 7% to 15% lower than $j^H(T_i)$.

TABLE II. Evaporation flux for varying liquid temperature T_l and length of the non-thermostated region L_n that lead to almost the same interface temperature T_i.

L_n	T_l	T_i	$j \cdot 10^3$
5.2	0.8000	0.7705	4.504
10.4	0.8240	0.7740	4.523
15.6	0.8466	0.7712	4.496

Conclusion

We have found above 1) that the interface temperature T_i shows an asymptotic behavior as a function of the length of the non-thermostated region L_n, yielding a limiting temperature T_i^∞ and 2) that the evaporation flux j depends in essence only on T_i. By combining these two facts we estimate now the evaporation flux j^∞ for a macroscopically large non-thermostated region in which heat transport takes place. For the particular case of the bulk liquid temperature $T_l = 0.8$ or $T_l\,/T_c = 0.74$ we found $T_i^\infty = 0.6349$. Calculating the Hertz flux for this temperature yields $j^H(T_i^\infty) = 1.061 \cdot 10^{-3}$. Consulting Table I one can expect an effective value for the evaporation flux of $j^\infty = 0.987 \cdot 10^{-3}$ that is 7% below the Hertz flux.

Another route is to estimate j^∞ from simulation data by interpolation, using results of simulations that yield interface temperatures close to T_i^∞. Since it is common to perform evaporation simulations with rather short lengths of the non-thermostated region (which saves a lot of computation time) and varying the bulk liquid temperature, we also started our

TABLE III. Evaporation flux for varying bulk liquid temperature T_l and constant length $L_n = 1.5\delta$, where δ is the 10-90 thickness of the interface[45] in its equilibrium state.

T_l	T_i	$j \cdot 10^3$
0.625	0.6214	0.801
0.650	0.6447	1.098
0.675	0.6677	1.483

study in the very beginning by performing such simulations for a temperature range from $T_l = 0.625$ to 0.950 in 13 steps ($\Delta T = 0.025$) and a length of the non-thermostated region of $L_n/\delta = 1.5$, where δ is the 10-90 thickness of the interface[45] in

the equilibrium state. Table III shows the relevant extract of those results. Interpolation between the corresponding values yields $j^{\infty} = 0.973 \cdot 10^{-3}$.

Against the background that the evaporation flux is solely determined by the interface temperature T_i, we want to incorporate a third way to estimate j^{∞} in this discussion by correlating the evaporation flux with the interface temperature T_i. For that purpose, we used the results presented in Table I (columns 2 and 4) and found the correlation

$$\mathrm{j}(\mathrm{T_i}) = \mathrm{b} \cdot \exp(\mathrm{cT_i}), \tag{4}$$

with $b = 4.14 \cdot 10^{-7}$ and $c = 12.12$. This approach yields $j^{\infty} = 0.910 \cdot 10^{-3}$. We correct this value according to a deviation of 8.7% that correlation (4) shows for the results of simulation with $L_n = 208$, cf. Table I, i.e. $j^{\infty} = 0.989 \cdot 10^{-3}$.

As an average over the outcomes of the three routes to estimate the particle flux for a macroscopically large non-thermostated region, i.e. for $L_n \to \infty$, we obtain $j^{\infty} = 0.983 \cdot 10^{-3}$. Finally, we want to compare this value to the Hertz flux with respect to the bulk liquid temperature $T_l = 0.8$ as it is usually done to obtain the evaporation coefficient

$$\alpha = \mathrm{j} \,/\, \mathrm{j^H}(\mathrm{T_l}). \tag{5}$$

With the Hertz flux $j^H(T_l = 0.8) = 7.058 \cdot 10^{-3}$ we obtain an evaporation coefficient of $\alpha = 0.14$.

The present result for α amounts only to $\approx 20\%$ of the values given in a review[22] of literature data, where the heat transfer to the interface was not explicitly taken into account. Moreover, we should still mention that Eames et al.[31] also conjectured that heat transfer limitations can have a considerable influence on experimental evaporation rates, and thus apparent evaporation coefficients, which is in line with the present calculations.

Supplementary Material

For better visibility, profiles for $L_n = 208$ are omitted in Figure 2 of the present manuscript. These omitted profiles are shown in an extended version of this plot as supporting information in the supplementary material.

ACKNOWLEDGEMENTS

This work was partly financed by Deutsche Forschungsgemeinschaft (DFG) under grant number VR 6-9/2 as an associated project to SFB-TRR 75 "Droplet Dynamics Under Extreme Ambient Conditions". The simulations were performed at the High Performance Computing Center Stuttgart (HLRS) under the grant MMHBF2. One of us (JF) gratefully acknowledges fruitful discussions over the years with Professor H.K. Cammenga, TU Braunschweig, Dr. M. Faubel, Max-Planck-Institut für Dynamik und Selbtsorganisation Göttingen, and Dr. K. Hammeke, Forschungszentrum Jülich.

REFERENCES

[1]H. Hertz, Ann. Phys. **253**, 177 (1882).

[2]M. Knudsen, Ann. Phys. **352**, 697 (1915).

[3]W. Prüger, Z. f. Physik **115**, 202 (1940).

[4]K. Leven, Wärme- und Kältetechnik **44**, 161 (1942).

[5]K. Hammeke, Ein pyrometrisches Verfahren zur Messung der Oberflächentemperatur von Wasser bei Verdampfungsversuchen. – Ein Beitrag zur Bestimmung des Kondensationskoeffizienten von Wasser. Ph.D. thesis, Universität Münster, Germany (1955).

[6]K. Hammecke and E. Kappler, Z. f. Geophysik **19**, 181 (1953).

[7]H. Cammenga, Zur Kinetik des Überganges kondensierte Phase / Dampf. Habilitation thesis, Technische Universität Braunschweig, Germany (1972).

[8]K. Hickman and W. Kayser, J. Colloid & Interf. Sci. **52**, 578 (1975).

[9]U. Narusawa and G.S. Springer, J. Colloid & Interf. Sci. **50**, 392 (1975).

[10]M. Faubel, S. Schlemmer and J.P. Toennis, Z. f. Physik D **10**, 269 (1988).

[11]G.T. Barnes and D.S. Hunter, J. Colloid & Interf. Sci. **88**, 437 (1982).

[12]C.A. Ward and D. Stanga, Phys. Rev. E **64**, 051509 (2001).

[13]S. Popopov, A. Meling, F. Durst and C.A. Ward, Int. J. Heat Mass Transf. **48**, 2299 (2005).

[14]V.K. Badam, V. Kumar, F. Durst and K. Danov, Exp. Therm. Fluid Sci. **32**, 276 (2007).

[15]F. Bošnjaković, Technische Mechanik und Thermodynamik **1**, 358 (1930).

[16]G.T. Barnes and H.K. Cammenga, J. Colloid & Interf. Sci. **72**, 140 (1979).

[17]S.I. Anisimov and A.Kh. Rakhmatulina, Zh. Eksp. Teor. Fiz. **64**, 869 (1973) [Sov. Phys. JETP **37**, 441 (1973)].

[18]J. Fischer, Phys. Fluids **19**, 1305 (1976).

[19]S.S. Sazhin, I.N. Shishkova, A.P. Kryukov, V.Yu. Levashov and M.R. Heikal, Int. J. Heat Mass Transf. **50**, 2675 (2007).

[20]A. Frezzotti, L. Gibelli and S. Lorenzani, Phys. Fluids **17**, 012102 (2005).

[21]A. Lotfi, Molekulardynamische Simulationen an Fluiden: Phasengleichgewicht und Verdampfung, Fortschritt-Berichte VDI 3/335, VDI-Verlag Düsseldorf, 1993.

[22]A. Lotfi, J. Vrabec and J. Fischer, Int. J. Heat Mass Transf. **73**, 303 (2014).

[23]V.V. Zhakhovskii and S.I. Anisimov, Zh. Eksp. Teor. Fiz. **111**, 1328 (1997) [Sov. Phys. JETP **84**, 734 (1997)].

[24]S.I. Anisimov, D.O. Dunikov, V.V. Zhakhovskii and S.P. Malyshenko, J. Chem. Phys.**110**, 8722 (1999).

[25] T. Ishiyama, T. Yano and S. Fujikawa, Phys. Fluids **16**, 2899 (2004).

[26] R. Hołyst and M. Litniewski, J. Chem. Phys. **130**, 074707 (2009).

[27] S. Cheng, J.B. Lechman, S.J. Plimpton and G.S. Grest, J. Chem. Phys. **134**, 22704 (2011).

[28] J. Yu and H. Wang, Int. J. Heat Mass Transf. **55**, 1218 (2012).

[29] T. Ishiyama, S. Fujikawa, T. Kurz and W. Lauterborn, Phys. Rev. E **88**, 042406 (2013).

[30] H. Cammenga, Evaporation mechanisms of liquids, in Current Topics in Materials Science, Vol. V/4, E. Kaldis (Ed.), North-Holland Publishing Company, Amsterdam, 1980, pp. 335-446.

[31] I.W. Eames, N.J. Marr and H. Sabir, Int. J. Heat Mass Transf. **40**, 2963 (1997).

[32] R. Marek and J. Straub, Int. J. Heat Mass Transf. **44**, 39 (2001).

[33] M. Volmer, *Kinetik der Phasenbildung*, Steinkopff-Verlag, Dresden, Leipzig, 1939.

[34] R.W. Schrage, *A Theoretical Study of Interface Mass Transfer*, Columbia University Press, New York, 1953.

[35] M.N. Kogan, *Rarefied Gas Dynamics*, Plenum Press, New York, 1969.

[36] S. Fujikawa, T. Yano and M. Watanabe, *Vapor-Liquid Interfaces, Bubbles and Droplets*, Springer Verlag, Berlin, Heidelberg, 2011.

[37] S. Sazhin, *Droplets and Sprays*, Springer Verlag, London, 2014.

[38] C. Niethammer, M. Becker, M. Bernreuther, M. Buchholz, W. Eckhardt, A. Heinecke, S. Werth, H.-J. Bungartz, C.W. Glass, H. Hasse, J. Vrabec and M. Horsch, J. Chem. Theory Comput. **10**, 4455 (2014).

[39] J. Vrabec, G. Kedia, G. Fuchs and H. Hasse, Mol. Phys. **104**, 1509 (2006).

[40] M. Thol, G. Rutkai, R. Span, J. Vrabec and R. Lustig, Int. J. Thermophys. **36**, 25 (2015).

[41] R. Lustig, G. Rutkai and J. Vrabec, Mol. Phys. **113**, 910 (2015).

[42] B. Smit, J. Chem. Phys. **96,** 8639 (1992).

[43] W. Shi, J.K. Johnson, Fluid Phase Equilib. **187-188,** 171 (2001).

[44] M. Allen and D. Tildesley, *Computer Simulation of Liquids*, Oxford University Press, New York, 1987.

[45] J. Lekner and J. Henderson, Physica A **94**, 545 (1978).

Supplementary material to:

Communication: Evaporation – Influence of heat transport in the liquid on the interface temperature and the particle flux

by

Matthias Heinen,[1] Jadran Vrabec,[1,a)] and Johann Fischer[2]

[1]*Lehrstuhl für Thermodynamik und Energietechnik, Universität Paderborn, Warburger Str. 100, 33098 Paderborn, Germany*

[2]*Institut für Verfahrens- und Energietechnik, Universität für Bodenkultur, Muthgasse 107, 1190 Wien, Austria*

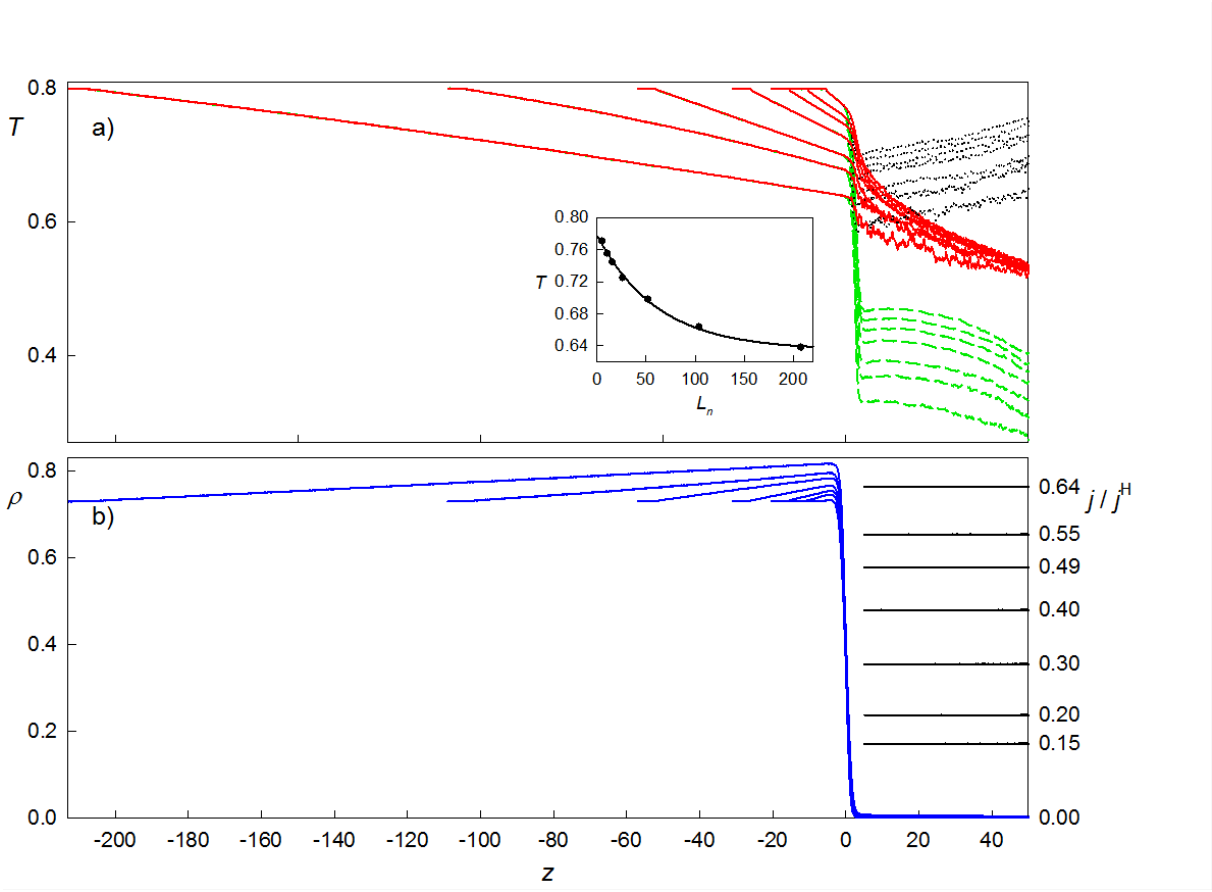

FIG. S1. Profiles obtained at $T_l = 0.8$ for different lengths of the non-thermostated region $L_n = 5.2, 10.4, 15.6, 26, 52, 104$ and 208. a) Temperature components T_{xy} (solid red), T_z (dashed green) and kinetic energy e (dotted black lines) which coincide in the liquid up to the interface boundary. The inset shows the interface temperature T_i vs. L_n. Bullets indicate simulation data and the line shows correlation (3). b) Density ρ (blue) and evaporation flux j (black lines) normalized to the Hertz flux j^H for $T_i = 0.8$.